Spatial imaging of individual vibronic states in the interior of single molecules

Q. Huan,[1,2] Y. Jiang,[1,3] Y. Y. Zhang,[2] U. Ham,[1] and W. Ho[1,a)]
[1]*Department of Physics and Astronomy and Department of Chemistry, University of California, Irvine, California 92697–4575, USA*
[2]*Institute of Physics, Chinese Academy of Sciences, Beijing 100190, China*
[3]*International Center for Quantum Materials, Peking University, Beijing 100871, China*

(Received 1 August 2010; accepted 18 May 2011; published online 6 July 2011)

Selective excitations of specific vibronic modes in position space are realized in single naphthalocyanine molecules adsorbed on an ultrathin alumina film by a scanning tunneling microscope at low temperature. Distinct spatial distributions are imaged for the different vibronic modes, which are in accordance with spectra recorded over different points of the molecule and its orbital structure. These distinct vibronic images, together with the differential conductance images and calculated molecular orbitals, lead to vibrational excitations that are associated with the doubly degenerate lowest unoccupied molecular orbitals (LUMO) – LUMO-α and LUMO-β. These results reveal the presence of different molecular conformations on the surface and the nature of the electron-vibrational coupling.
 [doi:10.1063/1.3598958]

Molecular vibrations are associated with many physical, chemical, and biological processes.[1,2] Investigation of molecular vibrations at the atomic scale provides insights into the chemical and electronic structures of the molecule and their coupling to the local environment. Results from these studies are of fundamental importance in molecular science and additionally have potential applications in single-molecule based devices.[3–5]

Because of its highly confined tunneling current, scanning tunneling microscope (STM) has been used to excite and detect molecular vibrations through inelastic electron tunneling spectroscopy (IETS) with sub-Ångström precision.[6,7] Inelastic tunneling process occurs when the energy of the tunneling electron is higher than the threshold of excitation of a vibrational mode. In this process, the electron loses its energy and excites molecular vibrations, which is equivalent to the opening of an inelastic tunneling channel. Vibrations in the range of a few hundred meV near the Fermi level can be excited and detected with STM-IETS. For molecules on metal surfaces, the strong molecule-metal interactions broaden the vibronic progressions within the electronic states.

The introduction of a buffer layer, such as a molecular layer or an ultrathin insulating layer, can effectively reduce the coupling between the molecule and the metal surface and extend the lifetime of transient states. Consequently, the observation of vibronic progressions in different electronic states becomes possible. The buffer layer changes not only the coupling but also the physical structure of the tunneling junction, changing from a single-barrier to a double–barrier tunneling junction. Detailed explanation of tunneling through a double-barrier junction has been described elsewhere.[8,9] Vibronic spectroscopy with submolecular resolution, which has been performed with the STM on single molecules, enables the study of spatially resolved molecular dynamics involving electron-vibrational coupling within different molecular orbitals in single molecules.[10–14] The localization of molecular vibrations on single naphthalocyanine (NPc) molecules is revealed by recording spectra at different positions over the molecule.[14] These spectra are composed of several series of equally spaced peaks that are interpreted as progressions of molecular vibronic modes. However, the detailed spatial distribution of the peak intensity in different progressions, which was attributed to the spatial dependence of the coupling of electrons to different vibrational modes, remains unclear. A deeper understanding of the spatially dependent electron-vibrational coupling in two dimensions requires simultaneous imaging of the molecular orbital and the vibration corresponding to a specific vibronic progression, which cannot be obtained from spectroscopic mapping across the molecule.

In the present paper, we use spatially resolved spectroscopy and vibronic imaging to explore the vibrational distribution in the interior of single naphthalocyanine molecules adsorbed on an ultrathin Al_2O_3 film grown on the NiAl(110) surface. The spatial distributions of the vibronic modes in different electronic states of single naphthalocyanine molecules are compared to the simultaneously recorded electronics states and calculated molecular orbitals.

The experiments were carried out with a homemade ultra-high vacuum STM operated at 12 K with a base pressure better than 5×10^{-11} Torr.[15] The NiAl(110) surface was cleaned by repeated cycles of Ne sputtering and annealing. In order to obtain a uniform Al_2O_3 layer ($\sim$5 Å in thickness) on the clean NiAl(110) surface with a coverage about 50%,[16] we exposed NiAl(110) at 750 K to 150 Langmuirs of O_2, followed by annealing it to 1300 K. Naphthalocyanine molecules were deposited onto the surface at 12 K by thermal sublimation from the solid. Both the first and second harmonics

a)Author to whom correspondence should be addressed. Electronic mail: wilsonho@uci.edu.

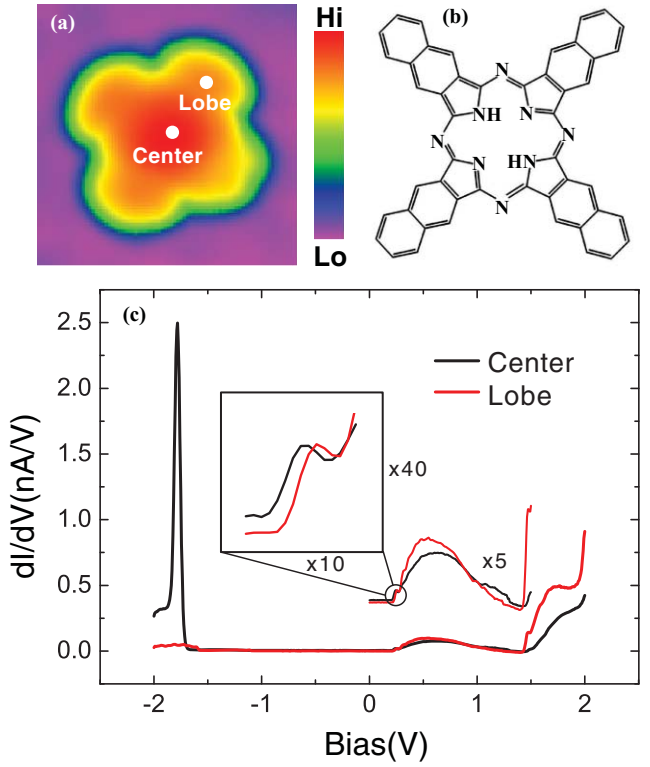

FIG. 1. (a) Constant current topographic image (4.25 nm × 4.25 nm) of a single naphthalocyanine (NPc) molecule adsorbed on an alumina layer on NiAl(110). Bias voltage is 1.30 V and tunneling current is 60 pA. (b) Schematic of the NPc molecule. (c) dI/dV spectra of the NPc molecule measured at the center (black) and the lobe (red) of the molecule, as shown in (a); tunneling gap set at 1.30 V and 60 pA. The amplitude of the bias modulation was 10 mV rms. Inset shows the difference in the onset between the two spectra.

of the tunneling current were recorded simultaneously with the lock-in technique while keeping the feedback loop open and applying a modulation voltage at ~260 Hz with root-mean-square amplitude of 7–15mV to the sample bias. The differential conductance (dI/dV) and vibronic (d^2I/dV^2) images were obtained in a similar way as the constant current topographic (z) images. The tunneling current and its harmonics were recorded at each point for a chosen bias with feedback turned off. The bias corresponding to a vibronic peak is often different than that chosen for setting the constant current.

The topographic images and dI/dV spectra reveal different conformations for the naphthalocyanine molecules adsorbed on the alumina surface. Figure 1 shows the topographic image [Fig. 1(a)] and the dI/dV spectra [Fig. 1(c)] of a molecule with the conformation that is common and very stable on the oxide surface. Different from previous results,[14] the molecules with this conformation have one lobe [lower right lobe in Fig. 1(a)] that is distinctly different from the other three lobes in the topographic image. Spectra taken at the center and on the upper right lobe of the molecule further reveal the molecular electronic states. As is shown in Fig. 1(c) two bands are observed at positive sample bias, which can be assigned to the LUMO and the LUMO+1, respectively. The onset of the LUMO lies in the range of 0.15 V–1.0 V, depending on the adsorption site. For some conformations, only the LUMO is observed in the scanned voltage range. In Fig. 1(c) the onsets of the LUMO and LUMO+1 are ~0.2 V and ~1.4 V, respectively.

Instead of the highest occupied molecular orbital (HOMO) state, we observed within the scanned voltage range only a sharp peak at negative sample bias in the center of the molecule that is absent on the lobe. The ratio of the conductance onsets for the sharp peak to the LUMO is ~8.2, which is close to the ratio (7.1±2.6) of the conductance onsets of CuPc molecules.[8] The sharp peak at negative bias in Fig. 1(c) is attributed to the onset of bipolar conduction through the LUMO when it is pulled below the Fermi level in a double-barrier tunnel junction. The ratio of the conduction onsets is approximately given by $\varepsilon z/d$, where ε is the effective dielectric constant of the oxide film (~8 for bulk alumina), z is the tip-molecule distance, and d is the oxide layer thickness.[8] As is shown in the inset of Fig. 1(c), the onset of the LUMO in the center of the molecule is slightly lower than that on the lobe, and this difference is also exhibited in the d^2I/dV^2 spectroscopic mapping across the molecule [Fig. 2(d)]. This onset shift, which is attributed to the combined effects of the alumina layer inhomogeneity, the tip height difference [Fig. 2(b)], and variation of the molecule-substrate interaction, is responsible for the absence of the sharp peak on the molecular lobe in the scanned voltage range. According to the double-barrier tunneling model, the shift of the LUMO at positive bias is expected to be 25 to 100 times smaller than that of the sharp peak at negative bias.[9] The sharp peak on the lobe should be located within −2.20 V to −3.20 V.

Spatial variation of the LUMO and its vibronic states can be revealed by a series of dI/dV and d^2I/dV^2 spectra measured at different positions over a single naphthalocyanine molecule (Fig. 2). The spectroscopic mapping was taken at equally spaced positions marked from 1 to 11 in Fig. 2(a). Fine steps are observed in the dI/dV spectra [Fig. 2(c)], which correspond to different vibronic progressions. The position and height of the steps in the dI/dV spectra change along the molecule. These changes can be more clearly analyzed in the d^2I/dV^2 mapping [Fig. 2(d)]. The d^2I/dV^2 spectra consist of a series of peaks which are associated with different vibronic progressions. Every peak shows variation in intensity along the molecule. The shift of the peak onset is less than 10 mV, due largely to the tip height change [Fig. 2(b)] across the molecule.

Here we use the d^2I/dV^2 spectra to show the vibronic features of the molecule, while noting that it is the dI/dV spectra that are of physical significance in inelastic tunneling and vibronic tunneling. The relation between dI/dV and d^2I/dV^2 spectra is shown in Fig. 3 Assume that the peaks in the dI/dV spectra are Gaussians: $f(x) = Ae^{-(x-a)^2/2\sigma^2}$, the corresponding d^2I/dV^2 curve would have maxima that scales with the maxima in the dI/dV peaks, i.e., if max(dI/dV) = A, then $\max(d^2I/dV^2) = 1/\sqrt[2]{e*\sigma^2} * A = \text{constant} * A$. The maximum in the intensity for each peak in the d^2I/dV^2 spectrum is proportional to the maximum in the slope of the dI/dV peak at its inflection point. It should be noted that the inflection point is displaced from the peak in the dI/dV by a constant (σ) and the intensity at the inflection point is

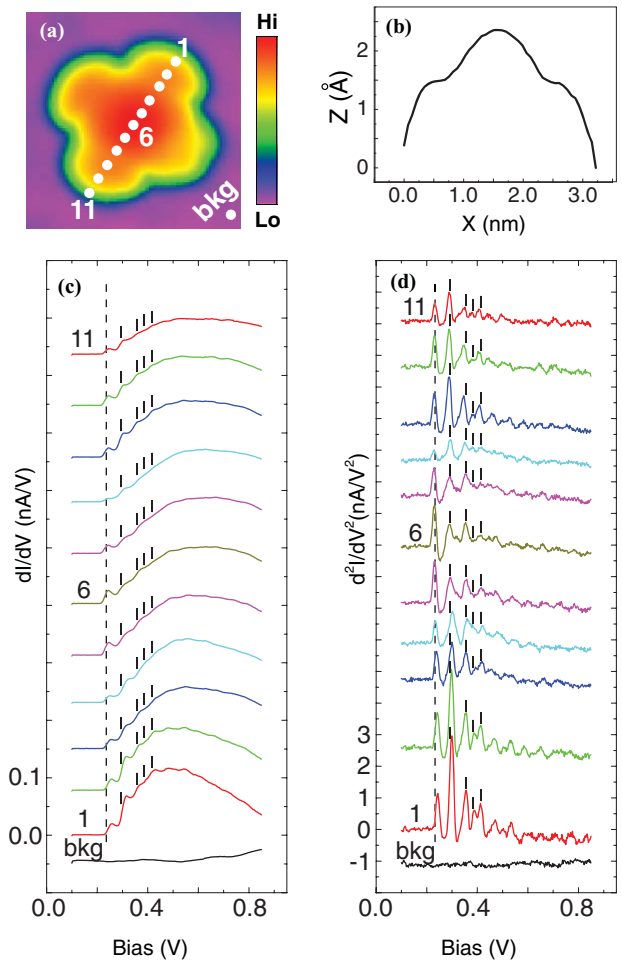

FIG. 2. (a) Constant current topographic image with dots corresponding to the positions over the molecule where dI/dV and d^2I/dV^2 spectroscopic mapping were recorded. (b) Tip height profile of the molecule from point 1 to point 11 in (a). (c) dI/dV spectroscopic mapping and (d) d^2I/dV^2 spectroscopic mapping taken across a naphthalocyanine molecule at equally spaced positions from 1 to 11, as shown in (a). The background (bkg) curves were recorded over the oxide away from the molecule, as shown in (a). The set point for the tunneling gap was 1.30 V and 60 pA; the bias modulation was 7 mV. The spectra are offset for clarity.

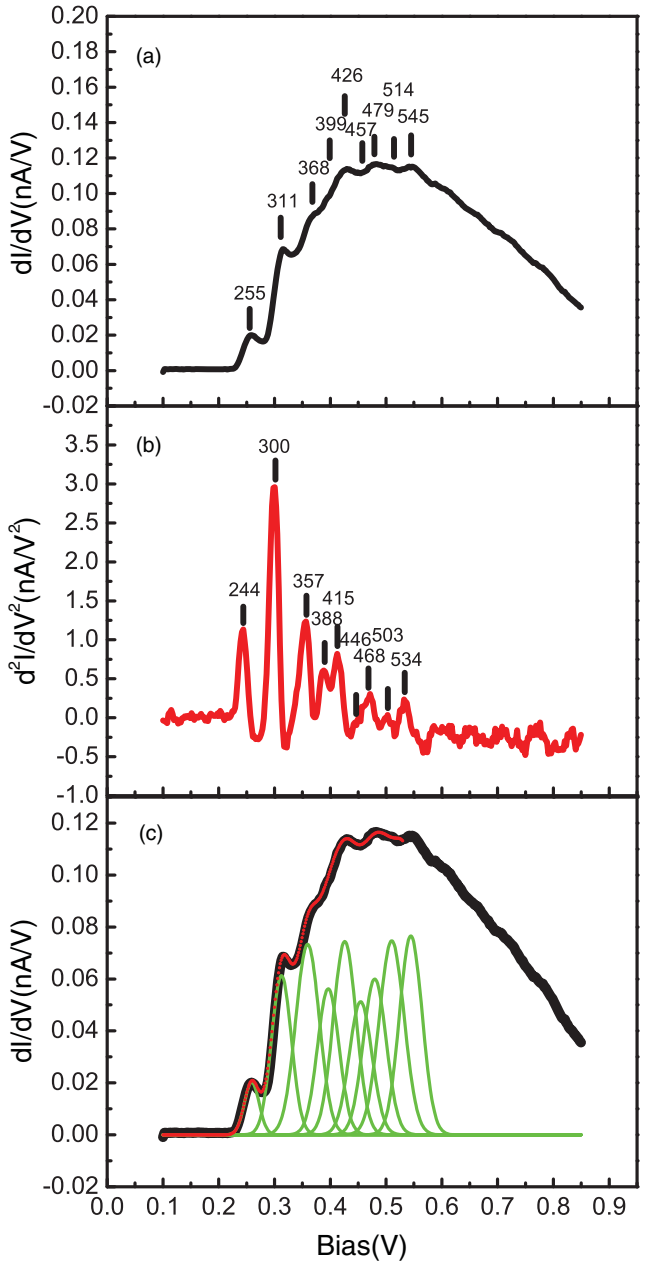

FIG. 3. Correspondence of peak positions in the dI/dV spectrum (a) and the d^2I/dV^2 spectrum (b) [taken at point 1 in Fig. 2(a)]. (c) Fitting of the dI/dV spectrum (red dotted curve) is composed of summing a series of Gaussion peaks (green) centered at the positions marked in (a).

[1/sqrt(e)]A = constant*A. Figure 3(c) is the fitting of the dI/dV spectrum with a series of Gaussian peaks at positions shown in Fig. 3(a).

The d^2I/dV^2 spectra were fit with multiple sequences of equally spaced Gaussian peaks constrained to have the same linewidth; several vibronic progressions can be resolved.[17] Figure 4 shows the fitting results for the spectra at the center of the molecule [position 6, Fig. 4(a)] and on the lobe [position 9, Fig. 4(b)]. Eighteen Gaussian peaks were used to perform the fitting for each spectrum, and six vibronic progressions can be assigned (red, magenta, blue, light magenta, cyan, and light cyan in colors). Every progression is composed of a few peaks with a common separation of 121 ± 3 mV (Fig. 5), which can be assigned to one vibronic progression. All six progressions exhibit two types of spatial variations over the molecule. The first type, which includes the red, magenta, and light magenta progressions, has relatively strong intensity in the center of the molecule and become weaker on the lobe. However, the second type, which includes the blue, cyan, and light cyan progressions, shows the opposite trend. This spatial distinction between the vibronic progressions was also observed for the LUMO lying further (by ~0.6 V) above the Fermi level of the substrate.[14] For the same type of progressions, the spatial dependence of the peak intensity shows the same trend but differs in the magnitude of the change in the intensity from one peak to another.

Vibrational motions of single molecules reveal the interrelationship among the molecular conformations, the vibronic modes, and the molecular orbital structure. To further understand the spatial dependence of the electron-vibrational coupling and to explain the origin of the spatial variation of different vibronic progressions, we performed the imaging of

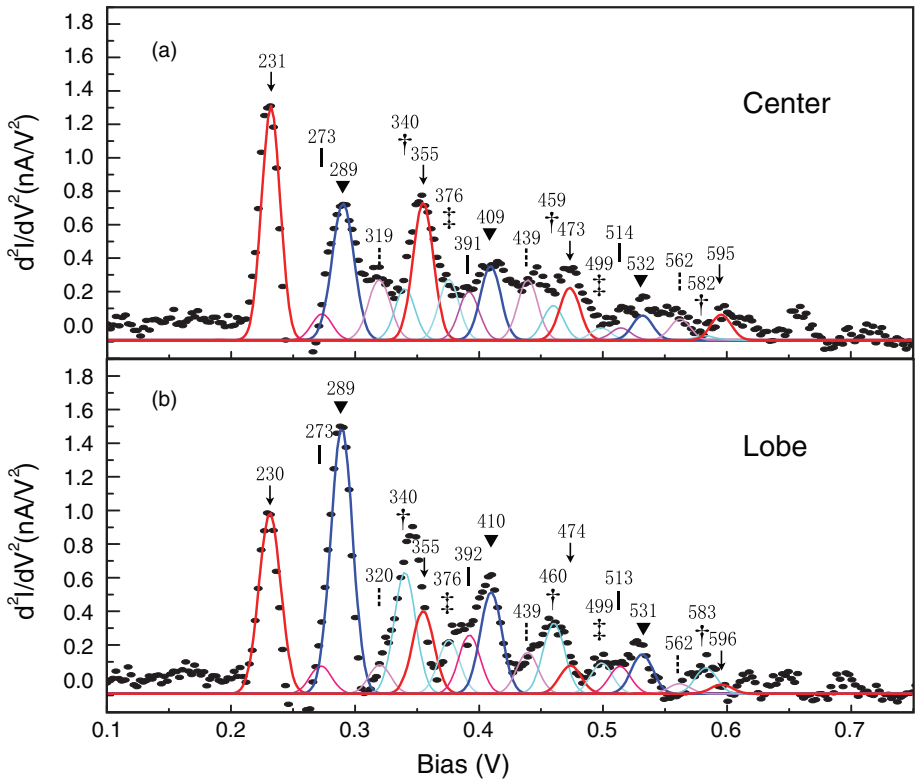

FIG. 4. Peak fittings of the d^2I/dV^2 spectra with series of equally spaced Gaussion peaks. (a) Over the center [point 6 in Fig. 2(a)] and (b) the lobe (point 9). The Gaussian peaks are assigned to different progressions which are distinguished by line fits and peak indicators in different colors. The red (↓), magenta (|), and light magenta (¦) progressions are within the LUMO-α, while the LUMO-β contains the blue (▼), cyan (†), and light cyan (‡) progressions.

the individual vibronic modes and the molecular orbital with sub-Ångström resolution. The vibrational and the molecular orbital images are obtained simultaneously by recording the d^2I/dV^2 and dI/dV signals at every pixel with a sample bias aligned with a particular vibronic mode within an electronic state. The d^2I/dV^2 image taken at the voltage corresponding to the peaks in d^2I/dV^2 (the inflection point in dI/dV) is directly proportional to the dI/dV image taken at the voltage corresponding to the peak in dI/dV. In this way, we could obtain with high resolution the spatial distribution of the vibronic modes and molecular orbital.

Figures 6(a) and 6(b) show the vibronic (d^2I/dV^2) images and the molecular orbital (dI/dV) images obtained at several sample biases on the same molecule. The biases are indicated by a dashed line (229 mV) or short bars (other voltages) in the dI/dV mapping [Fig. 2(c)] and the d^2I/dV^2 mapping [Fig. 2(d)]. At 229 mV, which correspond to the first peak in the d^2I/dV^2 spectra, the d^2I/dV^2 and dI/dV images show similar patterns. These patterns, referred to as "type I", follow closely to a two-fold symmetry and contain nodal structure. The dI/dV image at 288 mV [Fig. 6(b2)] closely follows that at 229 mV, except that all the lobes become more intense. However, the pattern for the d^2I/dV^2 image at 288 mV is rotated by 90° and is denoted as "type II". As the bias increases, the orientation and symmetry of the patterns in the dI/dV and d^2I/dV^2 images do not appear to change, except for an overall increase in the intensity.

In order to understand the molecular orbital structure and how it affects the electron-vibrational coupling based on the dI/dV and d^2I/dV^2 images acquired at different biases, we carried out density functional theory (DFT) calculations of the orbitals for the free NPc molecule, as shown in Fig. 6(c). The structure of the NPc molecule was fully relaxed. The DFT calculations use the Perdew-Wang functional (PW91),[18] ultrasoft pseudopotentials,[19] and a plane wave basis set as implemented in the PWSCF code.[20] A 30 × 30 × 15 Å^3 supercell was used to model the isolated NPc molecule. The electronic wave functions were expanded in plane waves with a kinetic energy cutoff of 400 eV and were sampled at the Gamma point. The structure was relaxed until residual forces were less than 0.01 eV/Å. As can be seen from the schematic structure [Fig. 1(b)] and the ball-and-stick model [Fig. 6(c3)] of the molecule, NPc molecule is planar and has four-fold symmetry if the two hydrogen atoms in the middle are deleted. The existence of two hydrogen atoms, as seen by their tautomerization,[22] breaks the four-fold symmetry and the degeneracy of the electronic states. The LUMO and the LUMO+1 split into two and four states, respectively, in the presence of the two hydrogen atoms. Calculations suggest that the two LUMO states, LUMO-α and LUMO-β, are separated by ~90 meV. Within the Tersoff-Hamann approximation,[21] we simulated the dI/dV images for LUMO-α [Fig. 6(c1)] and LUMO-β [Fig. 6(c2)] by integrating the electron density of these two states over an energy interval of 20 meV. In the calculation, the two hydrogen atoms are located along the direction joining the upper left to the lower right of the molecule, as shown in Fig. 6(c3). The LUMO-β has the same pattern as the LUMO-α but is rotated

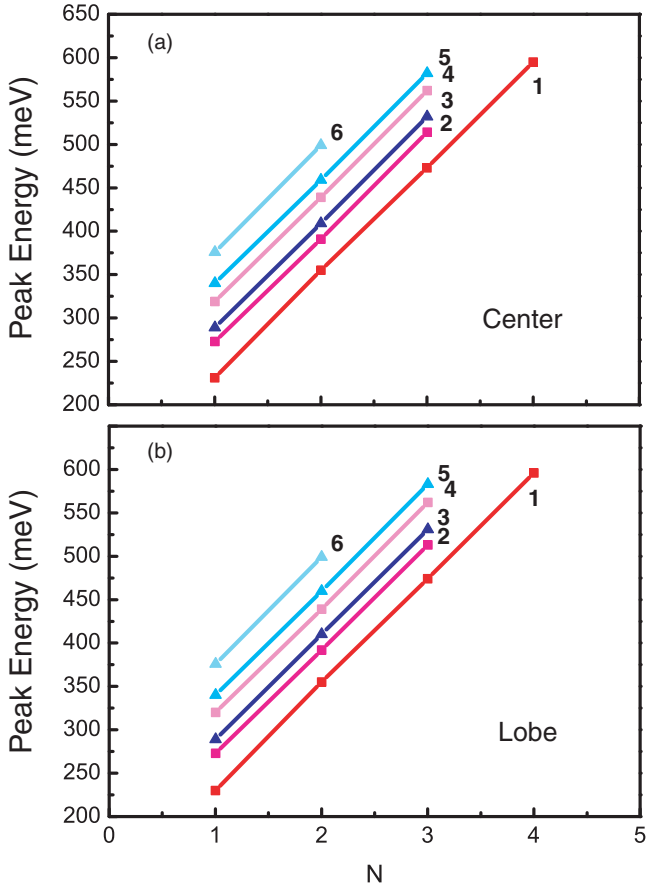

FIG. 5. Vibronic peak energy vs. the peak number obtained from the spectra of NPc over (a) the center [point 6 in Fig. 2(a)] and (b) the lobe (point 9). The solid lines depict the linear fits for extracting the vibrational energies from the slopes of the different progressions. (a) 1: 121.0 ± 0.8 mV, 2: 120.5 ± 1.4 mV, 3: 121.5 ± 0.9 mV, 4: 121.5 ± 0.9 mV, 5: 121.0 ± 1.2 mV, 6: 123.0 mV. (b) 1: 121.7 ± 0.8 mV, 2: 120.0 ± 0.6 mV, 3: 121.0 ± 0.5 mV, 4: 121.0 ± 1.2 mV, 5: 121.5 ± 0.9 mV, 6: 123.0 mV. The colors of the solid lines correspond to the colors of different progressions in Fig. 4. Square and triangular correspond to progressions within LUMO-α and LUMO-β, respectively. The energy difference between LUMO-α and LUMO-β is 57±3 mV in (a) and (b). For the progressions on progressions within LUMO-α and LUMO-β, shifts of 42 ± 2 mV and 87 ± 3 mV (referenced to the main red sequence) and shifts of 50 ± 2 mV and 88 ± 2 mV (referenced to the main blue sequence) were observed.

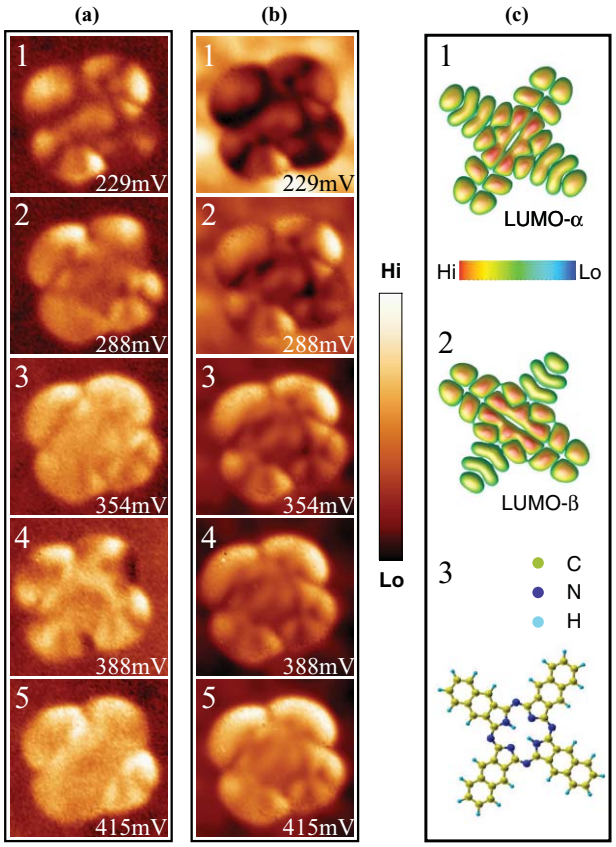

FIG. 6. Spatial distribution of (a) vibronic intensity, d^2I/dV^2 images and (b) electronic density of states, dI/dV images, obtained simultaneously for different biases modulated at 15 mV, with the gap set at bias of 1.30 V and tunneling current of 60 pA. (c) Calculated LUMO-α (c1) and LUMO-β (c2) of free naphthalocyanine molecule and the ball-and-stick model (c3) of the molecule.

by 90° in the molecular plane. It is possible to distinguish the LUMO-α and the LUMO-β even though the molecule is adsorbed strongly on the surface. The bonding may be electrostatic due to the polar surface and thus may not involve much rehybridization of the orbital. The spatial distribution and symmetry of the LUMO-α and LUMO-β correspond to the type I and type II patterns in the d^2I/dV^2 images.

Based on the above spectroscopic data, dI/dV and d^2I/dV^2 images, and calculated molecular orbitals, a deeper understanding of the electron-vibrational coupling at the submolecular scale can be obtained. Because the LUMO-α and LUMO-β of naphthalocyanine molecule are close to each other in energy, the first band in the positive bias side of the dI/dV spectra in Fig. 1(c) is a mixture of two states. However, the dI/dV image at the onset of the band shows features that are consistent with the LUMO-α. When the sample bias is increased from 229 mV, the LUMO-β starts to contribute and the dI/dV image at 415 mV [Fig. 6(b5)] is composed of an admixture of the LUMO-α and LUMO-β. By comparing the type I (type II) d^2I/dV^2 images at 229 mV (288 mV) with the calculated LUMO-α and LUMO-β, the molecular structure and the positions of the two hydrogen atoms can be determined from the topographic and spectroscopic images. We did not observe tautomerization as reported by Liljeroth *et al.*[22] It could be that the molecule is more strongly bonded on the surface and hence tautomerization can only occur at higher bias voltages which may disrupt bonds in the molecule or change molecule conformation.

The spatial imaging and spectroscopic mapping of the individual vibronic states and the comparison with DFT calculations enable the assignment of the vibronic progressions. The common peak spacing of 121±3 mV in the main sequence can be assigned to the naphthalene breathing mode (111 meV).[23,24] Since the red and the blue sequences are the lowest vibronic progression of the LUMO-α and LUMO-β (Fig. 5), the energy difference of ~60 meV between these two sequences represents the energy separation of the LUMO-α and LUMO-β, which closely compares with ~90 meV from the calculation. The degeneracy of the LUMO-α and LUMO-β is lifted due to adsorption. Furthermore, the assignment of peaks belonging to the other progressions within the same molecular orbital should be referenced to these two

progressions (so called progression on progression[17]). For the progressions within the LUMO-α (red, magenta, and light magenta sequences) and LUMO-β (blue, cyan, and light cyan sequences), shifts of 42 ± 2 mV and 87 ± 3 mV (referenced to the main red sequence) and shifts of 50 ± 2 mV and 88 ± 2 mV (referenced to the main blue sequence) were observed, respectively. The two lower energy modes correspond to vibrations in the far-infrared range, which are highly coupled and difficult to be assigned.[24] The two higher energy modes can be assigned to the Pc breathing or pyrrole skeletal distortion vibrations (84 meV).

It is necessary to point out that our results are not inconsistent with previous results reported in Ref. 12. Because of the conformation difference and surface inhomogeneity,[25] which can be confirmed by the topographic images and the onsets of spectra, the molecules in the two studies exhibit different electronic and vibronic characters. Further understanding of the interactions between the molecules and the surface and how they affect molecular states and vibrations require calculations for a large unit cell of the oxide surface, which is beyond this paper. Moreover, it is difficult to resolve simultaneously the atomic structure of the oxide surface and the molecular structure since the imaging conditions are quite different.

An electron from the STM tip first tunnels resonantly into a vibronic state of the molecular orbital, and possibly involving the excitation and relaxation of a vibrational mode of a transiently charged molecule. When the electron leaves the molecule and tunnels into the substrate, the molecule returns to its neutral state and may be vibrationally excited. The localized vibronic modes could be accessed non-locally through the delocalized π–electron state of the organic molecule. Therefore, the spatial images for the different vibronic modes show the spatial distribution of the molecular orbital containing the modes. According to the Franck-Condon principle, the vibronic transitions between two LUMO states can be ruled out due to their poor overlap.

Excitation and detection of spatially dependent vibronic states in naphthalocyanine have been previously reported by recording spectra at different positions over a molecule.[12] However, spectroscopy alone could not resolve the nearly degenerate molecular orbitals because only a small number of positions were sampled. Since the nearly degenerate molecular orbitals are close in energy, they overlap with each other and only show one single band in the dI/dV spectra. Electrons tunnel into the vibronic states of the LUMO-α or LUMO-β, thus these two states cannot be distinguished from each other by either dI/dV imaging or spectroscopic mapping. Spectroscopic imaging, as reported in this paper, enables the measurement of the spatial distribution of individual vibronic states within an electronic state over many positions of the molecule. With spectroscopic imaging, it has become possible to probe electron-vibrational coupling in-depth and resolve closely separated molecular orbitals that are sensitive to the different conformations and the adsorption environment.

We also carried out spectroscopic mapping and vibronic imaging for the LUMO+1. Vibronic progressions can also be observed within the LUMO+1, but the FWHM of the peaks is wider than that of the LUMO. Larger peak shift ($\sim$30 mV) is observed for the vibronic peaks within the LUMO+1 in the spectroscopic mapping at different positions over the molecule. Because of the large peak shift, it is difficult to analyze the vibrational images due to contributions from neighboring vibronic peaks at a selected bias.

In summary, we investigated the spatial distributions of individual vibronic states in single naphthalocyanine molecules adsorbed on an ultrathin alumina grown on a NiAl(110) substrate by spectroscopic mapping and imaging. The variations in the images of the electronic states and vibronic progressions of the molecule at different sample biases, combined with DFT calculations, reveal that the vibrations in the LUMO arise from two nearly degenerate molecular orbitals, LUMO-α and LUMO-β. A separation of $\sim$60 meV in energy has been measured between these two states. The spatial distribution and symmetry of the vibronic modes are related to those of the molecular orbitals containing the modes.

This work was supported by the National Science Foundation (NSF) under Grant No. DMR-0606520. The authors are grateful to X. Chen, X. H. Qiu, and S. W. Wu for inspiring discussions.

[1] *Vibrational Spectroscopy of Molecules on Surfaces*, edited by J. T. Yates and T. E. Madey (Plenum, New York, 1987).
[2] *Modern Molecular Photochemistry*, edited by N. J. Turro (Benjamin/Cummings, Menlo Park, CA, 1978).
[3] C. Joachim, J. K. Gimzewski, and A. Aviram, Nature (London) **408**, 541 (2000).
[4] A. Nitzan and M. A. Ratner, Science **300**, 1384 (2003).
[5] S. Alavi, B. Larade, J. Taylor, H. Guo, and T. Seideman, Chem. Phys. **281**, 293 (2002).
[6] B. C. Stipe, M. A. Rezaei, and W. Ho, Science **280**, 1732 (1998).
[7] W. Ho, J. Chem. Phys. **117**, 11033 (2002).
[8] S. W. Wu, G. V. Nazin, X. Chen, X. H. Qiu, and W. Ho, Phys. Rev. Lett. **93**, 236802 (2004).
[9] G. V. Nazin, S. W. Wu, and W. Ho, Proc. Natl. Acad. Sci. U.S.A. **102**, 8832 (2005).
[10] X. H. Qiu, G. V. Nazin, and W. Ho, Phys. Rev. Lett. **92**, 206102 (2004).
[11] N. Liu, N. A. Pradhan, and W. Ho, J. Chem. Phys. **120**, 11371 (2004).
[12] N. A. Pradhan, N. Liu, and W. Ho, J. Phys. Chem. B **109**, 8513 (2005).
[13] H. J. Lee, J. H. Lee, and W. Ho, ChemPhysChem **6**, 971 (2005).
[14] N. Ogawa, G. Mikaelian, and W. Ho, Phys. Rev. Lett. **98**, 166103 (2007).
[15] B. C. Stipe, M. A. Rezaei, and W. Ho, Rev. Sci. Instrum. **70**, 137 (1999).
[16] R. M. Jaeger, H. Kuhlembeck, H.-J. Freund, M. Wuttig, W. Hoffmann, R. Franchy, and H. Ibach, Surf. Sci. **259**, 235 (1991).
[17] *Spectra of Polyatomic Molecules*, edited by G. Herzberg (Van Nostrand Reinhold, New York, 1966).
[18] J. P. Perdew, J. A. Chevary, S. H. Vosko, K. A. Jackson, M. R. Pederson, D. J. Singh, and C. Fiolhais, Phys. Rev. B **46**, 6671 (1992).
[19] D. Vanderbilt, Phys. Rev. B **41**, 7892 (1990).
[20] P. Giannozzi, S. Baroni, N. Bonini, M. Calandra, G. L. Chiarotti, M. Cococcioni, I. Dabo, A. D. Corso, S. de Gironcoli, S. Fabris, G. Fratesi, R. Gebauer, U. Gerstmann, C. Gougoussis, A. Kokalj, M. Lazzeri, L. Martin-Samos, N. Marzari, F. Mauri, R. Mazzarello, S. Paolini, A. Pasquarello, L. Paulatto, C. Sbraccia, S. Scandolo, G. Sclauzero, A. P. Seitsonen, A. Smogunov, P. Umari, and R. M. Wentzcovitch, J. Phys. Condens. Matter **21**, 395502 (2009).
[21] J. Tersoff and D. R. Hamann, Phys. Rev. B **31**, 805 (1985).
[22] P. Liljeroth, J. Repp, and G. Meyer, Science **317**, 1203 (2007).
[23] S. M. Arabei, J.-P. Galaup, K. N. Solovyov, and V. F. Donyagina, Chem. Phys. **311**, 307 (2005).
[24] I. Gobernado-Mitre, R. Aroca, and J. A. DeSaja, Chem. Mater. **7**, 118 (1995).
[25] G. H. Simon, T. König, H.-P. Rust, M. Heyde, and H.-J. Freund, New J. Phys. **11**, 093009 (2009).